International Journal of Aerospace and Lightweight Structures
Vol. 1, No. 2 (2011) 203–219
© Research Publishing Services
DOI: 10.3850/S2010428611000134

Analysis of Non-Linear Vibrations of Single-Layered Euler-Bernoulli Beams using Wavelets

Jan Awrejcewicz[1], Olga A. Saltykova[2,a], Maxim V. Zhigalov[2], Peter Hagedorn[3] and Vadim A. Krysko[2,b]

[1] *Department of Automation and Biomechanics, Technical University of Lodz, 1/15 Stefanowski Str, 90-924 Lodz, Poland.*
jan.awrejcewicz@p.lodz.pl

[2] *Department of Mathematics and Modeling Saratov State Technical University, 410054 Saratov, Politehnicheskaya 77, Russian Federation.*
[a] *olga_a_saltykova@mail.ru,* [b] *tak@san.ru*

[3] *SzM, Dynamics & Vibrations Group, LOEWE-Zentrum AdRIA, TU Darmstadt Bartning Str. 53, 64289 Darmstadt, Germany.*
peter.hagedorn@dyn.tu-darmstadt.de

Accepted 9 September 2011

In this work the investigation of non-linear vibrations of an Euler-Bernoulli beam for two types of boundary conditions has been carried out using the Gauss wavelets 1-8, and the Morlet wavelets. It has been shown that the latter ones give the most complete information about vibrations of the Euler-Bernoulli beams. In particular, the scenarios of transitions from a regular to chaotic beam dynamics are studied. In contrary to the standard approach based on the FFT (Fast Fourier Transform), the wavelets analysis allows following time evolutions of the beam frequency spectrum, and hence one may trace either an appearance or disappearance of frequency components. In addition, as it has been illustrated, the wavelet-oriented analysis allows us to investigate the redistribution of the beam energy over the frequency vibrations spectrum. Namely, we have shown how the beam energy located in a vicinity of the excitation frequency is transmitted into the other frequencies, when finally the system transits into the multi-frequency regimes.

Keywords: Bernoulli beams, Wavelets, Gauss function, Chaos.

1. Introduction

It is well known that vibrations of continuous systems play an important role in various applications, and hence this research has been challenging for many researchers over the years. There are numerous papers and books devoted to those types of problems including investigations of [Awrejcewicz and Krysko, 2003], [Awrejcewicz *et al.*, 2004, 2007], where a reader may found large lists of research references from both West and East countries. However, the approach presented in this paper is going beyond the classical investigations described in the mentioned monographs.

It rather extends our recent achievements associated with the analysis of continuous systems (beams, plates and shells) via wavelets. Recent results reported in references [Awrejcewicz and Krysko, 2008], [Krysko *et al.*, 2008a-d], concerning the Euler-Bernoulli and Timoshenko models are mainly focused on the investigation of the frequency power spectra of the studied vibration processes. In this work we apply different wavelet-functions like the Gauss wavelets 1, 8 and the Morlet wavelets, and in particular we analyse the influence of various boundary conditions on the beam regular and chaotic dynamics.

2. Mathematical Model

We are focused on the investigation of a single-layered beam being the 2D object in the space R^2 with rectangular co-ordinates introduced in the following way (Fig. 1) in the space $\Omega = \left\{x \in [0,a]\,;\, -h \le z \le h; -\frac{b}{2} \le y \le \frac{b}{2}\right\}$. The middle surface deformation is $\varepsilon_x = \frac{\partial u}{\partial x} + \frac{1}{2}\left(\frac{\partial w}{\partial x}\right)^2$, where $w(x,t)$ denotes the beam deflection, whereas $u(x,t)$ stands for its displacement along the ox axis.

The considered beam is subjected to the action of the following transversal load

$$q(x,t) = q_0 \sin(\omega_p t) \tag{1}$$

where ω_p is the excitation frequency, and q_0 is its amplitude. Recall that the classical theory of beams is founded on simplified assumptions introduced by Bernoulli (beams) and used by Kirchhoff and Love (plates and shells) regarding a normal to the investigated object middle surface: direct lines normal to the middle surface before deformation remain direct and normal to the middle surface and after deformation do not vary its length: $\varepsilon_{xx} = \varepsilon_x - z\frac{\partial^2 w}{\partial x^2}$, where ε_x is the

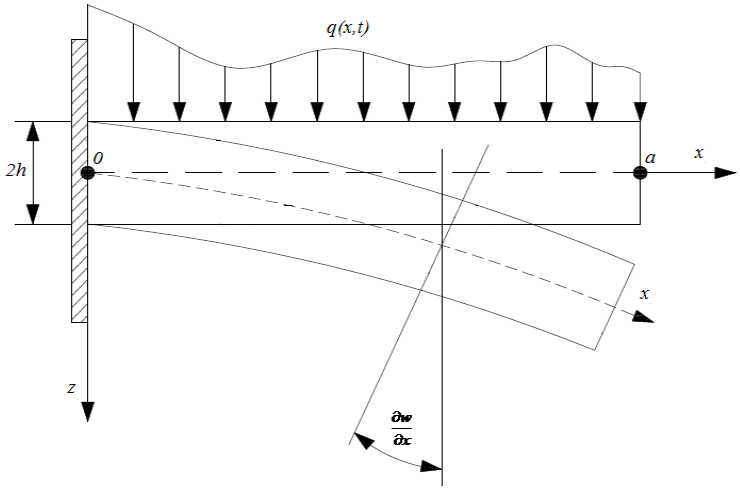

Fig. 1. Model of Euler-Bernoulli single-layered beam.

deformation in the direct line; $N_x = \int_{-h}^{h} \sigma_{xx} dz$ denotes a longitudinal force and $M_x = \int_{-h}^{h} \sigma_{xx}\, z\, dz = -\frac{(2h)^3}{12} E \frac{\partial^2 w}{\partial x^2}$ is a torque. In what follows the following system of dimensional equations are obtained:

$$\begin{cases} E\,(2h)\left\{\frac{\partial^2 u}{\partial x^2} + L_3(w,w)\right\} - (2h)\,\frac{\gamma}{g}\frac{\partial^2 u}{\partial t^2} = 0, \\ \\ E\,(2h)\left\{L_1(u,w) + L_2(w,w) - \frac{(2h)^2}{12}\frac{\partial^4 w}{\partial x^4}\right\} + q - (2h)\,\frac{\gamma}{g}\frac{\partial^2 w}{\partial t^2} - \varepsilon_1\,(2h)\,\frac{\gamma}{g}\frac{\partial w}{\partial t} = 0, \end{cases} \tag{2}$$

where $L_1(u,w) = \frac{\partial^2 u}{\partial x^2}\frac{\partial w}{\partial x} + \frac{\partial u}{\partial x}\frac{\partial^2 w}{\partial x^2}$, $L_2(w,w) = \frac{3}{2}\frac{\partial^2 w}{\partial x^2}\left(\frac{\partial w}{\partial x}\right)^2$, $L_3(w,w) = \frac{\partial^2 w}{\partial x^2}\frac{\partial w}{\partial x}$ are non-linear operators, ε_1 is a dissipative coefficient, $q = q(x,t)$ is a longitudinal load, E - Young module, and ρ, γ is a density and a weight density of the beam material, respectively, whereas g denotes the gravity acceleration. Since we do not take into account any dissipation within the beam material, a dissipation term regarding displacements (first equation of (2)) do not appear. Governing equations are reduced to the non-dimensional form using the following relations:

$$\begin{gathered} \bar{w} = \frac{w}{(2h_0)},\ \ \bar{u} = \frac{ua}{(2h_0)^2},\ \ \bar{x} = \frac{x}{a},\ \ \lambda = \frac{a}{(2h_0)},\ \ \bar{q} = q\frac{a^4}{(2h_0)^4 E}, \\ \bar{t} = \frac{t}{\tau},\ \ \tau = \frac{a}{c},\ \ c = \sqrt{\frac{Eg}{\gamma_1}},\ \ \bar{\varepsilon}_1 = \varepsilon_1 \frac{a}{c}. \end{gathered} \tag{3}$$

Taking into account (3), we obtain

$$\begin{cases} \frac{\partial^2 u}{\partial x^2} + L_3\,(w,w) - \frac{\partial^2 u}{\partial t^2} = 0, \\ \\ \frac{1}{\lambda^2}\left\{L_2(w,w) + L_1\,(u,w) - \frac{1}{12}\frac{\partial^4 w}{\partial x^4}\right\} - \frac{\partial^2 w}{\partial t^2} - \varepsilon_1 \frac{\partial w}{\partial t} + q = 0, \end{cases} \tag{4}$$

where in equations (4) bars are already omitted.

System (4) should be supplemented by one of the following boundary conditions.

- Clamping:

$$w(0,t) = w(a,t) = u(0,t) = u(a,t) = \frac{\partial w\,(0,t)}{\partial x} = \frac{\partial w\,(a,t)}{\partial x} = 0. \tag{5}$$

- Simple support:

$$w(0,t) = w(a,t) = u(0,t) = u(a,t) = \frac{\partial^2 w\,(0,t)}{\partial x^2} = \frac{\partial^2 w\,(a,t)}{\partial x^2} = 0. \tag{6}$$

The following initial condition is taken

$$w(x,t)_{|t=0} = \left.\frac{\partial w(x,t)}{\partial t}\right|_{t=0} = u(x,t)_{|t=0} = \left.\frac{\partial u(x,t)}{\partial t}\right|_{t=0} = 0. \tag{7}$$

3. The Finite Difference Method (FDM) and the Finite Element Method (FEM)

The problem of reliability and validity of the obtained results is important while studying nonlinear vibrations of the system in different regimes (periodic, quasi-periodic and chaotic ones). Since practically there is no hope to apply analytical methods of solving systems of nonlinear differential equations, the validity and reliability of computations are verified checking a correlation of the results obtained by different numerical methods. In this regard our numerical computations have been carried out using two methods: finite differences method (FDM) with $O(c^2)$ approximation and finite elements method (FEM) in the Bubnov-Galerkin form.

The infinite problem (4)–(7) will be solved via the FDM with the approximation of $O(c^2)$, and it is reduced to a system of ordinary differential equations (ODEs). In each node of a mesh the following set of ODEs is obtained:

$$\begin{cases} L_{1,c}(w_i(t), u_i(t)) + q_i(t) = \varepsilon_1 \dot{w}_i(t) + \ddot{w}_i(t); \\ \\ L_{2,c}(w_i(t), u_i(t)) = \ddot{u}_i(t); \quad (i = 0, ..., n), \end{cases} \tag{8}$$

where n denotes the partition number regarding a spatial coordinate, c is the computational step regarding spatial coordinate, and $L_{1,c}(w_i(t), u_i(t))$, $L_{2,c}(w_i(t), u_i(t))$ are difference operators. Additionally, the system of equations (8) is supplemented by the following equations on the boundary

$$w_0 = 0; \quad w_n = 0; \quad u_0 = 0; \quad u_n = 0. \tag{9}$$

Initial conditions for all mentioned boundary conditions have the following difference forms

$$w(x_i)_{|t=0} = 0; \quad u(x_i)_{|t=0} = 0; \quad \dot{w}(x_i)_{|t=0} = 0; \quad \dot{u}(x_i)_{|t=0} = 0, \ (i = 0, ..., n). \tag{10}$$

Construction methods of FEM discrete models are divided into two large groups. The first one uses minimization of different power functional; the second group is based on the variants of weighed disclosure. One of these variants is the Bubnov-Galerkin method [Krysko *et al.*, 2008d].

The obtained system of equations with the supplemented boundary and initial conditions is solved by the fourth order Runge-Kutta method.

4. Numerical Investigations

One of the important problems which occur, while solving problems regarding the chaotic phenomena in mechanics, is that addressing the reliability of obtained results. Since the differential equations governing behavior of the applied mathematical models are essentially nonlinear, analytical solutions cannot be obtained, and hence validity of results of the numerical solution cannot be verified.

In this work, solutions obtained via FDM and FEM are compared. Note, that for either FEM or FDM the partitions are carried out regarding a spatial coordinate and time. We have tested various explicit methods including the Runge method. Based on these studies we may take reliable computational parameters regarding the space partition and the time step being then used in our computations. Let us present one of the numerical examples for the following fixed parameters: $\varepsilon_1 = 1$ (damping coefficient), $\omega_p = 6, 9$ (frequency of vibrations), $\lambda = a/2h = 50$ (geometrical parameter). Time step $\Delta t = 3.90625 \cdot 10^3$ and the space step $\Delta A = 0,025$ have been chosen from the stability condition of the obtained solutions with respect to the Runge principle. In Table 1 scales associated with vibration type vs. amplitude of excitation $q_0 \in [0.6 \cdot 10^4]$ (they are constructed only for one value of ω_p) and drawings $w_{\max}(q_0)$ are reported.

Table 1. Scales associated with vibration type vs. amplitude of excitation and the drawings $w_{\max}(q_0)$.

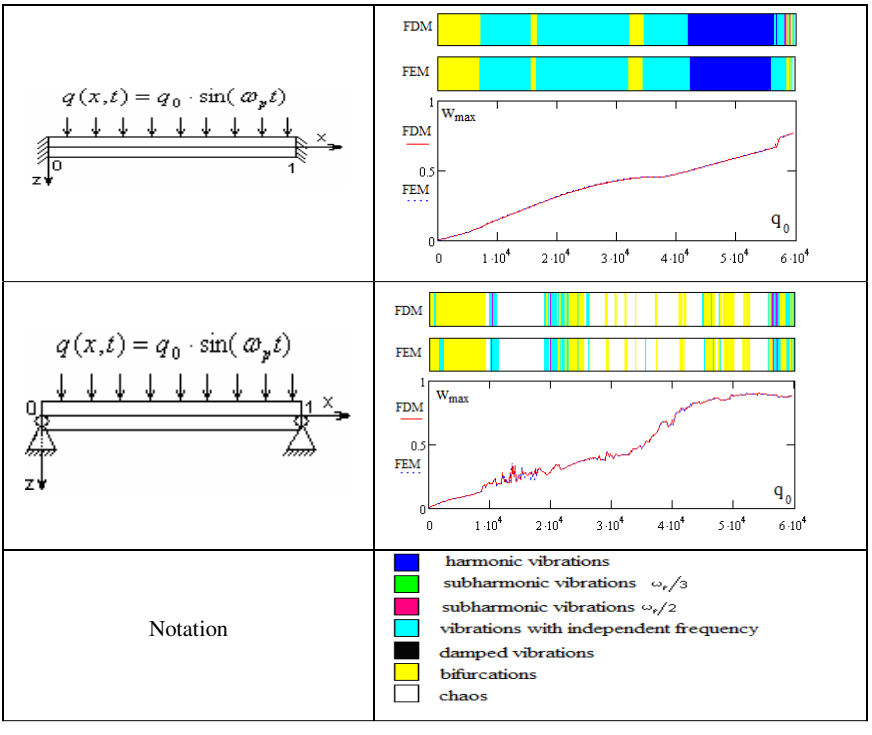

One may observe that different boundary conditions essentially influence a vibration regime of the investigated system. In the case of clamping, irrespectively of the numerical approach (FEM or FDM), the system exhibits independent frequency vibrations with zones of bifurcations. A transition to chaos is not observed in this case. In the graph $w_{\max}(q_0)$ sudden jumps and discontinuities are not observed. If

one considers zones regarding the simple support, then chaotic zones appear and they are interlaced with bifurcation zones. However, periodic zones are not detected at all in this case.

Observe that the dependence of maximum deflection vs. amplitude of excitation does not have sudden jumps of $w_{\max}$ only in the beginning (for $q_0 \in [0.\,1 \cdot 10^4]$). The transition from periodic to chaotic dynamics and vice versa is characterized by a sudden change of $w_{\max}$ corresponding to a simultaneous change of the amplitude of vibrations. This observation enables a definition of dynamical stability loss associated with transversal sign-changeable load action. All presented graphs have good convergence.

In other words the reported scales and graphs exhibit a convergence of the results of two applied methods. Functions of maximal deflection for boundary conditions (5) obtained either by FEM or FDM do not show essential differences for arbitrary values of excitation amplitudes. Investigated dynamical system does not achieve a chaotic regime. On the other hand, in the case of boundary conditions (6), presented scales and functions of the maximal deflection obtained by FEM and FDM differ slightly only in the case of chaos.

Table 2. Charts of dynamical regimes for different boundary conditions.

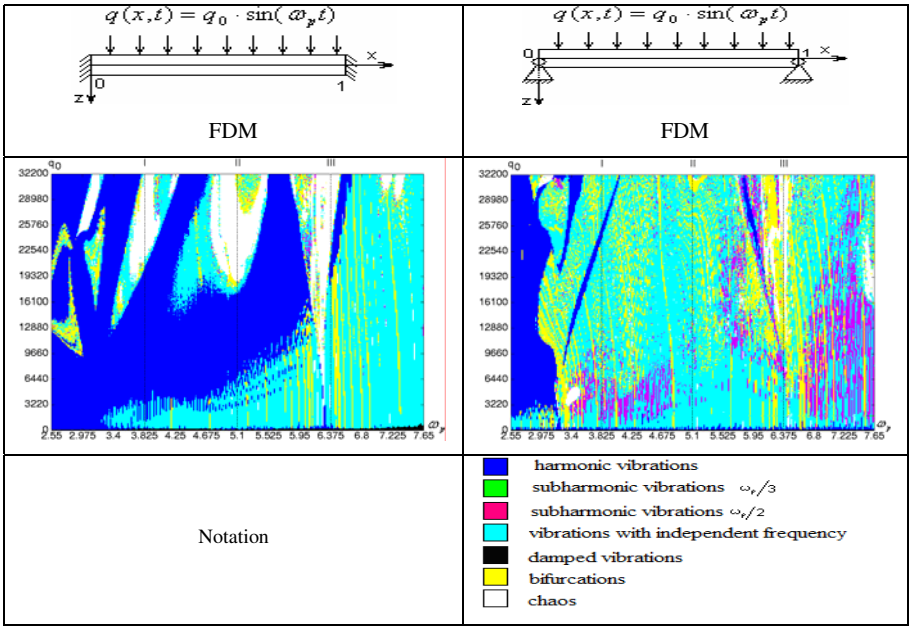

In order to investigate non-linear dynamics of the Bernoulli-Euler beams the so called maps of vibration regime depending on two control parameters $\{q_0, \omega_p\}$ are introduced. The maps represent a graphical transformation of the computational

results of the investigated dynamical systems. One of the important problems being addressed is that of getting full information of the system dynamics achieved via minimal computational time. The investigations of maps with the resolution of 100×100, 200×200, 300×300, 400×400 reported in reference [Krysko *et al.*, 2008d] indicate that the most optimal one is that of the resolution 300×300. However, to construct it one needs to compute and analyze $9{\cdot}10^4$ computational variants.

It should be emphasized that the computation with a Intel Core i3 processor, ram 2,0 Gb, CPU frequency 2,27 GHz using FDM with $n = 40$ requires the computational time of 50 days, whereas for $n = 80$ it needs 100 days. In the case of FEM application the computational time for the same case increases by about 1.5 to 1.7 times. Table 2 gives maps for boundary conditions (5) and (6) for the FDM.

Charts of the beam dynamical regimes allow yielding a prognosis of its vibration type regarding the chosen control parameters. As it is seen from reported charts, for the case of clamping-clamping for $q_0 < 16100$ and for $\omega_p < 5.95$ beam vibrations are either periodic or quasi-periodic. These regimes are not dangerous for construction exploitation. However, dangerous regimes referred as chaotic ones appear for large values of excitation amplitude and frequency. In the case of clamping-clamping areas of chaotic vibrations are rather represented marginally, however, the bifurcation phenomena play an important role in this case.

It is well known that in the case of identification and monitoring of regular and chaotic dynamics a key role plays the classical universal approach based on analysis of the frequency power spectrum of a being studied vibration process. In other words an application of the widely used in engineering FFT yields information of the system energy distribution. However, it possesses one essential drawback. Namely, it does not allow tracing temporal frequencies localization, which is very important characteristic while studying with time-dependent frequencies evolution. In order to remove the mentioned drawback one may apply a wavelet analysis.

Therefore, in this work, the time-frequency characteristics are reported with a use of the continuous wavelet transform proposed by Grossman and Morlet in the early 1980 [Krysko *et al.*, 2008d]. Nowadays, the literature devoted to wavelets is rather large so we restrict ourselves to mention the monographs [Krysko *et al.*, 2008a-c], [Grossman and Morlet, 1984], [Volmir, 1972], [Feigenbaum *et al.*, 1982], which could serve as a useful guide to continuous wavelet transform applications in engineering sciences. Application of the wavelet-type analysis can be found in references: [Staszewski *et al.,* 1998], [Staszewski, 1998], [Pernot *et al.,* 2001], [Pernot *et al.,* 2003], [Le *et al.,* 2004], [Erlicher *et al.,* 2007]. Investigation of the longitudinal deflection of flexible beams using the Haar wavelet is reported by [Lepik, 2011].

This novel field of analysis finds applications in signal processing and signal synthesis (for instance, in language recognition), in the analysis of transformations of various type, in investigation of the turbulent field properties, in finding solutions to equations, in pattern recognition, in human vision, image compression, radar and

earthquake prediction, de-noising of noisy data as well as in economical packing of large amount of information.

Area of application of the wavelet-type analysis is not limited to analysis of various signal properties obtained numerically either via an experiment or observation. Wavelets are also applied during the mathematical and computational modeling of a huge number of dynamics of non-linear processes exhibiting an interaction in a wide interval of both space and time scales. In particular, the wavelet-like analysis is very suitable for a study of essentially non-homogeneous processes, since its bases elements are well localized and possess a moving time-frequency window.

On the other hand, it is not known a priori, which wavelet type is most suitable to be applied for the analysis of chaotic vibrations of continuous systems. Therefore, numerical experiments are required in order to be sure about advantages of a wavelet-type choice. In addition, the carried out study should be supplemented by standard analysis like the FFT, phase projections (portraits), and Lyapunov exponents computations in order to choose the most adequate wavelet-type analysis of chaotic beam vibrations.

The wavelet-type studies are focused on a choice of the so-called *mother wavelet* or an *analyzing wavelet*. One mother (prototype) wavelet allows to perform the detailed frequency (low frequency version) and temporal (high frequency version) analysis of the data being investigated. This is achieved by using coefficients in a linear combination of the wavelet functions. Since a wavelet transformation is a scalar product of the analyzing wavelet and a signal under analysis, the coefficients $W(t, \omega)$ represent a combinational information on both wavelet and signal (the same is hold for the Fourier coefficients, which contain information on the signal and the sinusoidal wave). In this work in order to study chaotic vibrations of the Timoshenko beam we apply a few wavelet transforms and show that each of them possesses its own peculiar characteristic in time and frequency domains. Many researchers called the wavelet analysis "mathematical microscope" since the methods keeps good resolution on different scales. Parameter t concentrates the "mathematical microscope" focus, the scale coefficient ω allows to magnify the signal, and finally the "optical quality" of the microscope is defined via the choice of the basis wavelet ψ.

Real wavelet bases are often constructed using the Gauss function derivative

$$\psi_m(t) = (-1)^m \frac{\partial^m \left[\exp\left(-\frac{|t|^2}{2}\right)\right]}{\partial t^m}, \quad \widehat{\psi}_m(f) = m\,(if)^m \exp\left(-\frac{|f|^2}{2}\right) \tag{11}$$

where $\widehat{\psi}_m(f)$ is the Fourier transform.

A wavelet defined for $m = 1$ is called the WAVE – wavelet, whereas that for $m = 2$ is called MHAT – wavelet (Mexican hat). The Gauss wavelet for $m = 2$ has the narrow energy spectrum and two zero moments, whereas for $m = 8$ it has six zero moments and is better adjusted for chaotic signals analysis. Higher

order derivatives have more zero moments and allow to draw information on the peculiarities of higher order being hidden in the signal.

In many cases the applied basis is constructed using good localized in f and t the Morlet wavelet transform [Krysko *et al.*, 2008d], being a flat wave modulated by the Gaussian of unit width. Its wavelet function and its Fourier transformation follows:

$$\psi_m(t) = \exp(if_0 t)\exp\left(-\frac{|t|^2}{2}\right), \widehat{\psi}_m(f) = H(f)\exp\left(-\frac{(f-f_0)^2}{2}\right), \qquad (12)$$

where $H(f)$ is the Heaviside function. Observe that increasing of f_0 improves the angle selectivity, whereas the space selectivity is decreased.

Alongside with the Morlet wavelet, we have studied also other wavelets like the Gauss-1 (WAVE) and Gauss-8. The comparison of the results yielded by various wavelets applied will be given further during investigation of vibrations with the frequencies of $\omega = 7.0$.

The given results allow concluding that the chaotic vibrations essentially depend on the interval of changes of the control parameters. In this paper, we study peculiarities of the system transition from regular to chaotic states increasing the load amplitude for three excitation frequencies. A point in the control parameters space is denoted by $(\omega,\ q_0) \in \{\omega,\ q_0\}$. Frequency-temporal wavelet-spectra will be constructed using the following wavelets: Gauss wavelets of first and eighth orders and the Morlet wavelet.

Table 3. Investigations of the wavelet's type.

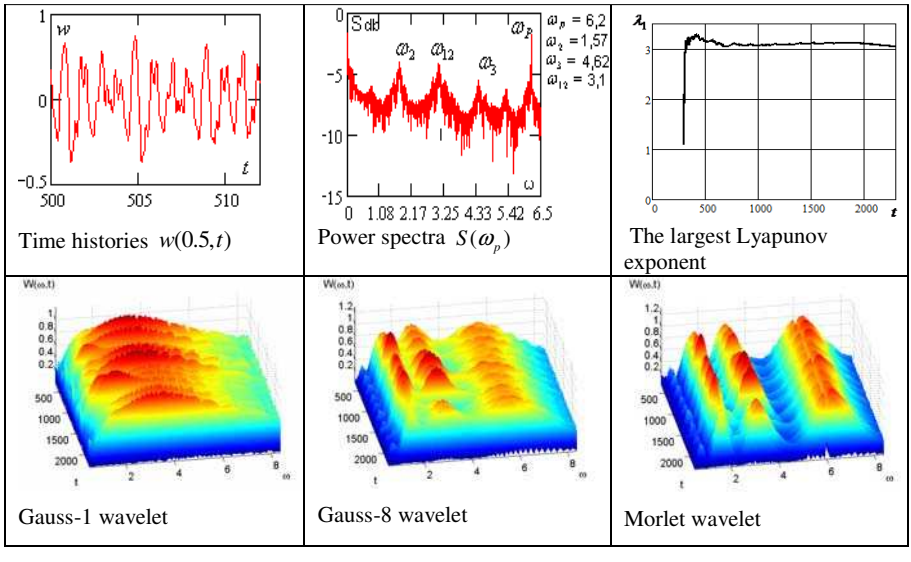

Let us consider the beam vibrations with $\omega_p = 6.2$ and $q_0 = 23500$ taking into account boundary conditions (5). The mentioned control point corresponds to beam chaotic vibrations. In Table 3 a time signal, a frequency power spectrum and a largest Lyapunov exponent λ_1 are reported. All of the mentioned characteristics indicate beam chaotic vibrations. In what follows we study various types of wavelets with respect to their advantages in direct and reliable investigation of the Euler-Bernoulli beam vibrations.

Although the increase of the Gauss wavelet order improves the obtained results, but even fort the Gauss-8 wavelet it is worse comparing with the used Morlet wavelet. Therefore, in the case of our Euler-Bernoulli beam the Morlet wavelet seems to be most optimal one. In order to analyse beam vibrations the following characteristics are applied:

(1) Time history (signal), i.e. a change of the beam deflection in time $w(t)$;
(2) Power spectrum of a vibration process on the basis of the Fourier transform (further referred as the Fourier-spectrum);
(3) Phase portrait, i.e. a curve in the phase plane $(w(t),\ dw(t)/dt)$;
(4) Poincare maps;
(5) Frequency-temporal 3D Morlet wavelet-spectrum;
(6) Windows in time ($t = 600$, 1400, 2200) of a 3D wavelet-spectrum.

Let us study a scenario of transition of our beam from regular to chaotic dynamics for $\omega_p = 6.2$ for boundary conditions (5). In further presented 3D Morlet wavelet-spectra the red (blue) colour corresponds to the maximum (minimum) beam energy.

(1) $q_0 = 50$. Harmonic vibrations with the excitation frequency $\omega_p = 6.2$ are clearly visible. One may distinguish in the wavelet-spectra that there exist frequencies in the low frequencies interval. Birth of the frequency $\omega_1 = 0,07$ is also remarkable, however, its role successively decrease in time.

    As it is seen from Table 4 the fundamental part of the beam energy is localized on the excitation frequency and the excitation frequency changes its position in different time instants. In time instant $t = 1400$ a new frequency $\omega = 5,7$ is born, which vanishes then. Therefore, the beam total energy changes in time. It should be emphasized that in the low-frequencies zone there is a series of frequencies, which do not change their positions in time but which are not reported through the Fourier spectrum. Poincare section corresponds to one point, which proves an occurrence of a periodic vibration.
(2) $q_0 = 10300$. In this case besides of the excitation frequency two more, i.e. $\omega_2 = 2,35$ and $\omega_3 = 3,85$, undergo evolutions in time. Since ω_P–$\omega_3 = \omega_2$, then ω_3 is treated as the dependent frequency. Then pair frequencies appear around ω_2 and ω_3. Their number increases up to a certain time instant, and then pair frequencies start to vanish. Furthermore, the frequencies values ω_P, ω_2 and ω_3 are not fixed, what is demonstrated by time cuts of the 3D wavelet-spectrum. Total system energy is divided between three frequencies ω_P, ω_3 and

Table 4. The scenario of transition into chaos.

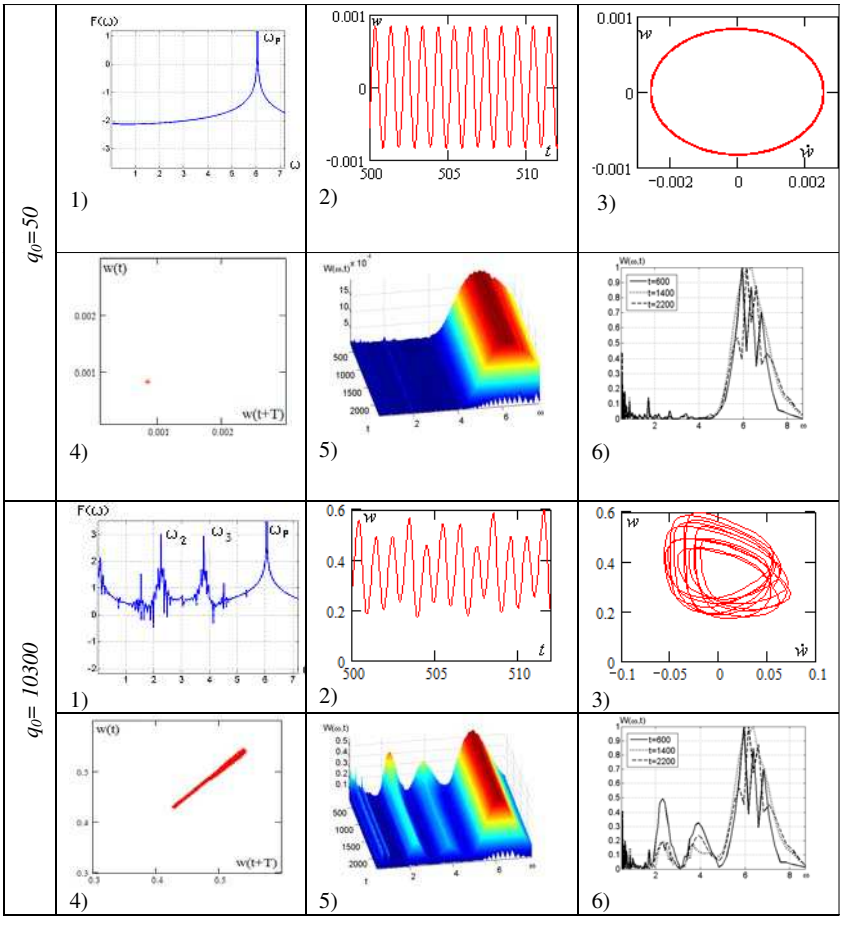

ω_2. Observe that the values of frequencies ω_2 and ω_3 for $t = 1400$ significantly differ from their counterpart values associated with different time instants.

(3) $q_0 = 16000$. In this case a reconstruction of the system frequencies takes place. A new frequency $\omega_4 = \frac{\omega_P}{2}$, around which the pair frequencies are localized, undergoes a period doubling bifurcation – I. Pair frequencies associated with the frequency ω_2 are ω_5 and ω_6; in the case of the frequency ω_4 the pair frequencies are ω_7 and ω_8; finally, in the case of ω_3 the pair frequencies are ω_9 and ω_{10}. Time history exhibits a quasi-periodic character, what is clearly illustrated on the phase portrait. Wavelet spectral frequencies $\omega_3 - \omega_{10}$ are overtaken by the fundamental frequencies $\omega_2, \omega_4, \omega_p$. In general, the total beam energy is localized in vicinity of ω_2. Poincare section exhibits an approximation to the attractor.

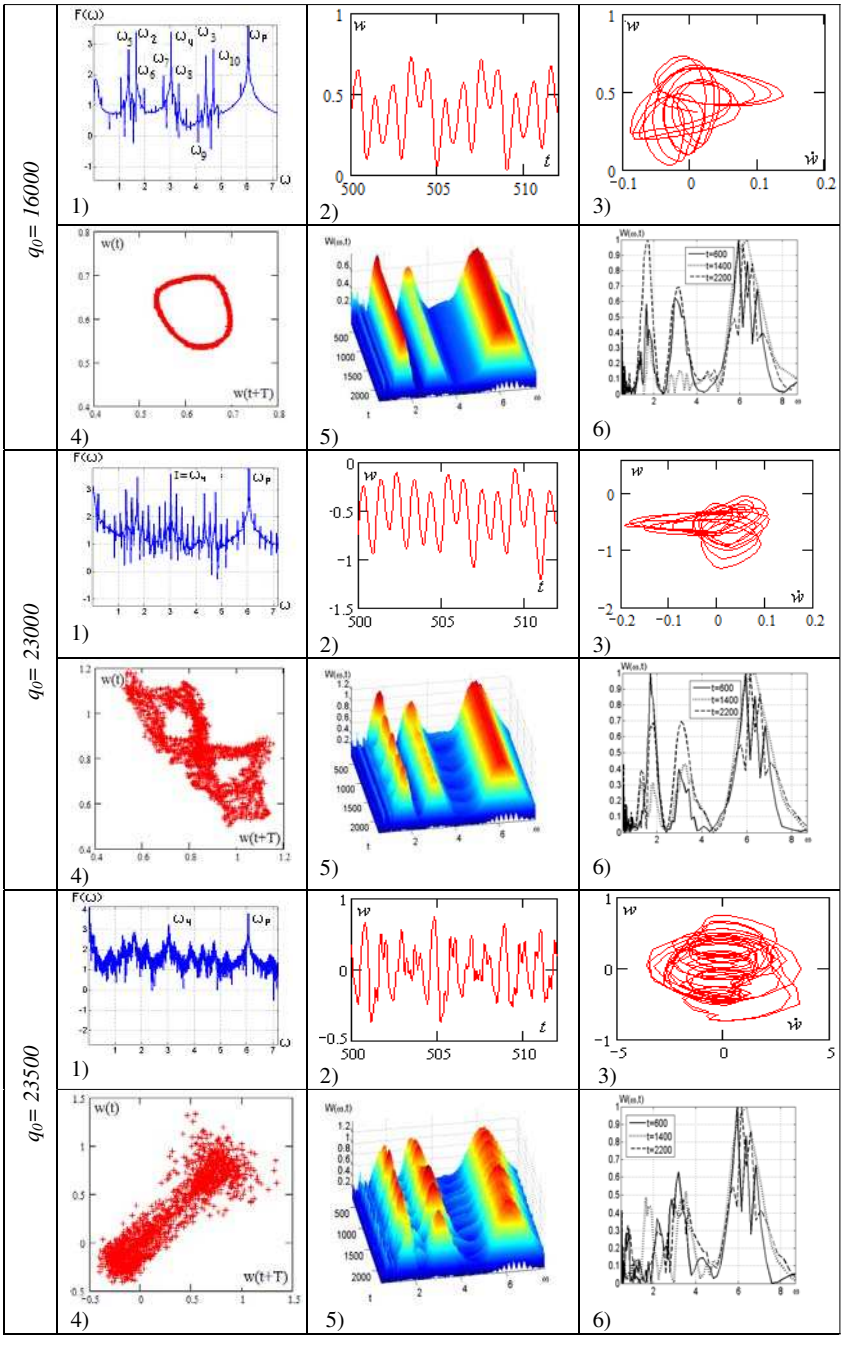

Time cuts of wavelet-spectra indicate that in initial time instant in the wavelet spectrum all frequencies exhibited by the Fourier spectrum appear. For $t = 2200$ only three frequencies ω_P, ω_2, ω_4 remain achieving their maximal values.

Table 5. The scenario of transition into chaos.

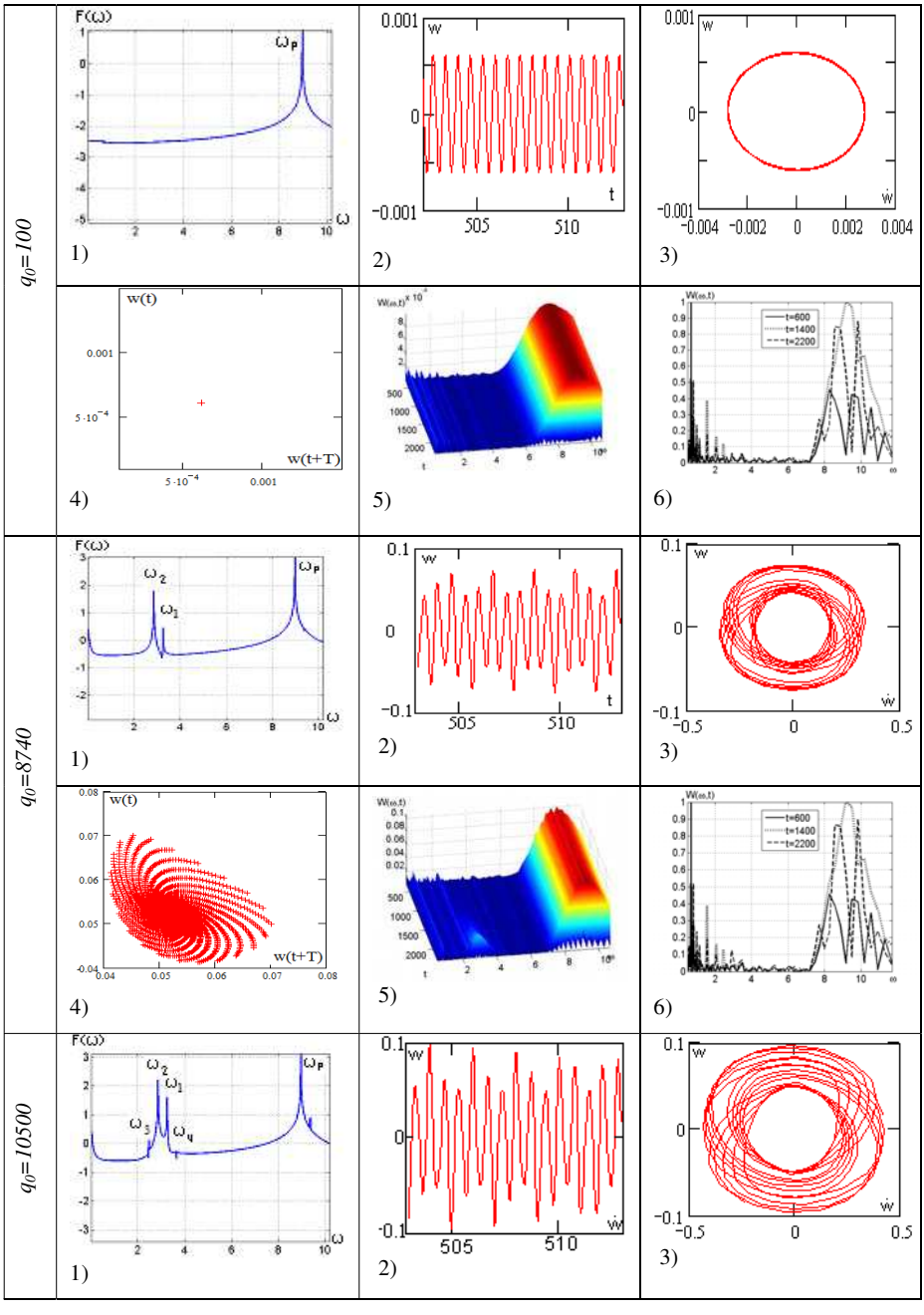

Further increase of the excitation load amplitude yields an increase of the number of pair frequencies.

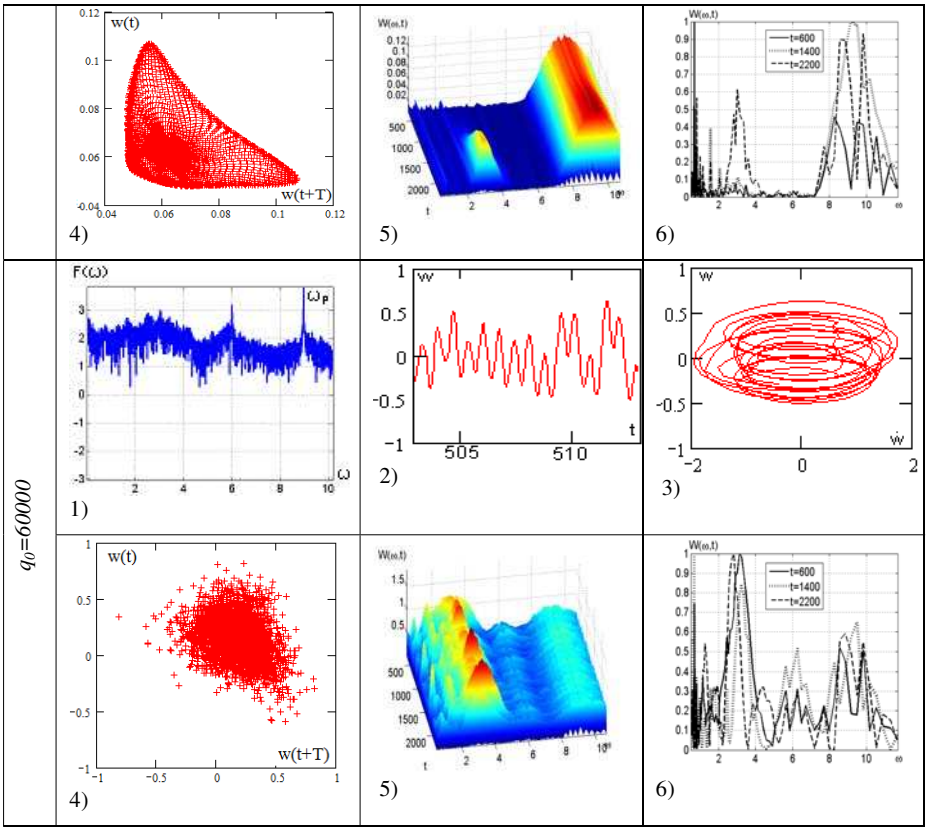

(4) $q_0 = 23000$. In this case wavelet-spectra indicate a multiple-frequency vibration character.

Maximum of the system energy is localized in the neighbourhood of the excitation frequency and ω_2 (for $t = 600$). Frequency ω_2 magnitude decreases in time, whereas the frequency $\omega_4 = \frac{\omega_P}{2}$ increases and at time instant $t = 2200$ both of them are equal.

(5) $q_0 = 23500$. In this case a frequency chaotic component occurs, and then the system starts vibrating chaotically. The wavelet-spectra exhibit chaotic vibrations with the dominating frequencies ω_2, ω_4 and ω_p. The system energy distribution is fully reconstructed, and the energy peak corresponds to the bifurcation frequency ω_4. Poincare section yields an approximation to the chaotic attractor.

Cuts of the wavelet spectra indicate that the frequencies positions and magnitudes essentially change in time. It is remarkable that on the long time intervals finally frequencies ω_2 and other ones decrease their magnitudes. Chaotic vibrations

are carried out on the excitation frequency, which means that it possesses the larger energy part.

In other words the scenario of transition into chaos can be understood as the modified Feigenbaum scenario with one independent frequency. In what follows we illustrate the scenario for the excitation frequency $\omega_p = 9.2$.

(1) $q_0 = 100$. Here the Fourier spectrum indicates occurrence of vibrations with the excitation frequency ω_P, and the output time history is harmonic. On the wavelet spectra one may distinguish a lot of "small" low value frequencies. System energy is localized on the excitation frequency. Cuts of the wavelet spectra demonstrate rather large oscillations of the frequencies magnitudes in time. Poincare section corresponds to one point, which proves an occurrence of a periodic vibration.

(2) $q_0 = 8740$. Increase of the excitation amplitude results in the successive occurrence of a first and second independent frequencies $\omega_1 = 3,31$, $\omega_2 = 2,92$. One may observe on the wavelet spectrum that the frequency $\omega_2 = 2,92$ having the largest energy component starts to appear for $t > 1500$. Observe that a so called energy pumping from the excitation frequency into interval of low frequencies occurs. A cut of the wavelet spectrum for the interval of frequencies in the neighbourhood of the excitation frequency is converged with the cut of the previous step. Poincare section exhibits a role of the irrational (independent) frequencies occurrence.

(3) $q_0 = 10500$. In this case one may recognize a birth of the third frequency $\omega_3 = 2,51$ and the fourth frequency $\omega_4 = 3,75$. Values of frequencies ω_1, ω_2 are decreased, and the following linear combination between the frequencies occurs: ω_1–$\omega_2 = \omega_2$-ω_3. Although the output time history becomes more complex, it still remains periodic. Increase of frequencies magnitude in time is evident, which is well documented by the wavelet spectrum cuts.

One may observe further the occurrence of a broad band spectrum being concentrated around frequencies ω_1, ω_2. The following linear combination of frequencies is observed: ω_1-$\omega_2 = \omega_2$-$\omega_3 = \omega_1$-ω_4, and the output signal amplitude increases. In the wavelet spectrum frequencies ω_1, ω_2 start to overlap owing to their previous close neighbourhood position. Further energy pumping is observed. It should be noted that the maximum of energy associated with frequencies ω_1, ω_2 and ω_p increases in comparison to its counter part value for $q_0 = 10500$.

(4) $q_0 = 60000$. In this case all applied characteristics like the Fourier spectrum, time history, phase portrait and wavelets spectra indicate a chaotic beam dynamics. System energy is mainly localized in the lower frequencies interval. Maximum energy values are achieved on frequencies ω_1, ω_2, i.e. in contrary to the previous scenario the excitation frequency does not play a crucial role in this transition to chaos. On the other hand observable changes of frequencies

in time are less comparing with the latter scenario, and this scenario can be referred to the quasi-periodic one.

5. Conclusions

Constructed charts of the beam vibration type allowed concluding that introduced boundary conditions play a crucial role on the beam dynamics. In addition the proposed charts are useful in direct application to constructions composed of beams and allow avoidance of dangerous regimes of vibrations.

After testing of various types of wavelets it has been proved that most adequate and suitable to the considered by us problem are the Morlet wavelets allowing tracing the frequency characteristics in time with a relatively high precision. On the other hand the application of the wavelet spectrum cuts allows following energy pumping with respect to external excitations.

Reported and described scenarios of transitions into chaos for the same beam but for different excitation frequencies show that the beam transition from regular to chaotic dynamics is realized via different scenarios.

Acknowledgements

J. Awrejcewicz acknowledges support of the Alexander von Humboldt Award during preparation of this work.

References

Awrejcewicz, J. and Krysko, V. A., [2003] *Nonclassical Thermoelastic Problems in Nonlinear Dynamics of Shells* (Springer, Berlin).

Awrejcewicz, J. and Krysko, V. A., [2008] *Chaos in Structural Mechanics* (Springer, Berlin).

Awrejcewicz, J., Krysko, V. A. and Krysko, A. V., [2007] *Thermo-Dynamics of Plates and Shells* (Springer, Berlin).

Awrejcewicz, J., Krysko, V. A. and Vakakis, P., [2004] *Nonlinear Dynamics of Continuous Elastic Systems* (Springer, Berlin).

Feigenbaum, M. J., Kadanoff, L. P. and Shenker, S. J., [1982] "Quasiperiodicity in dissipative systems: A renormalization group analysis", *Physica* V.D.5, 370.

Grossman, A. and Morlet, S., [1984] "Decomposition of Hardy functions into square separable wavelets of constant shape", *SIAM J. Math. Anal.*, **15**(4), 723.

Krysko, V. A., Zhigalov, M. V. and Saltykova, O. A., [2008a] "Nonlinear dynamics of the Euler-Bernoulli and Timoshenko beams", *Izvestiya Vuzov. Mashinostroenie*, **6**, 7–27, in Russian.

Krysko, V. A., Zhigalov, M. V. and Saltykova, O. A., [2008b] "Features of complex chaotic beams Euler-Bernoulli and Timoshenko type, depending on boundary conditions", *Izvestiya Vuzov. Stroitelstvo*, **9**, 4–10, in Russian.

Krysko, A. V., Zhigalov, M. V. and Saltykova, O. A., [2008c] "Management of complex nonlinear vibrations of multilayer beams", *Izvestiya Vuzov. Aviatsionnaya Technika*, **3**, 10–13, in Russian.

Krysko, V. A., Zhigalov, M. V., Saltykova, O. A. and Desyatova, A. S., [2008d] "The dissipative dynamics of geometrically nonlinear beams Bernoulli-Euler", *Izvestiya RAS. Mechanica Tverdogo Tela*, **6**, 128–136, in Russian.

Volmir, A. S., [1972] *Nonlinear Dynamics of the Plates and Shells* (Nauka, Moscow), in Russian.

Staszewski, W. J. and Worden, K., [1998] "Wavelet Analysis of Time Series: Coherent Structures, Chaos and Noise", special issue of the *International Journal of Bifurcation and Chaos*, **9**(3), 455–471.

Staszewski, W. J., [1998] "Identification of Non-Linear System Using Multi-Scale Ridges and Skeletons of the Wavelet Transform", *Journal of Sound and Vibration*, **214**(4), 639–658.

Pernot, S. and Lamarque, C. -H., [2001] "A wavelet-Galerkin procedure to investigate time-periodic systems: Transient vibration and stability analysis", *Journal of Sound and Vibration*, **245**(5), 845–875.

Pernot, S. and Lamarque, C. -H., [2003] "A wavelet-balance method to investigate the vibrations of nonlinear dynamical systems", *Nonlinear Dynamics*, **32**(1), 33–70.

Le, T.-P. and Argoul, P., [2004] "Continuous wavelet transform for modal identification using free decay response", *Journal of Sound and Vibration*, **277**, 73–100.

Erlicher, S. and Argoul, P. [2007] "Modal identification of linear non-proportionally damped systems by wavelet transform", *Mechanical Systems and Signal Processing*, **21**(3), 1386–1421.

Lepik, U., [2011] "Bucking of Elastic Beam by the Haar Wavelet Method", *Estonian Journal of Engineering*, **17**(3), 271–284.